THE JOURNAL OF PHYSICAL CHEMISTRY B

Article

pubs.acs.org/JPCB

Lifetime and Spectrally Resolved Characterization of the Photodynamics of Single Fluorophores in Solution Using the Anti-Brownian Electrokinetic Trap

Quan Wang[†,‡] and W. E. Moerner*[,†]

[†]Department of Chemistry and [‡]Department of Electrical Engineering, Stanford University, Stanford, California 94305, United States

ABSTRACT: We report simultaneous determination of fluorescence intensity, lifetime, and emission spectrum over time scales on the order of seconds for single molecules in solution, using the anti-Brownian electrokinetic trap. We demonstrate the technique with trapped single fluorophores of Atto647N and Alexa647. Three emission states with distinct intensities, lifetimes, and emission peaks are found in the case of Atto647N. Transitions between states happen occasionally. We characterize the three states and quantify the transition probabilities between states using concurrent intensity, lifetime, and spectrum data. Alexa647, on the other hand, showed little dynamics. These results represent a significant advance in the ability to identify and characterize different dynamical states of single molecules in aqueous solution with high precision and millisecond time resolution.

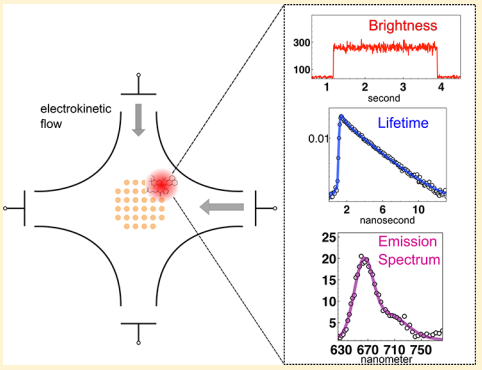

INTRODUCTION

Over the past decade, single-molecule techniques have evolved into powerful tools for scientists across different disciplines to tackle problems at the nanoscale.[1] Among these vastly diverse methods, optical detection of fluorescence provides a simple yet immensely powerful route to observe individual molecules.[2] It was realized early on in the field that different physical properties of the emitted fluorescence photons can be measured to extract different information about the single molecule or its local environment. For example, the polarization state of the fluorescence photons can be analyzed to report on the orientation of the molecular dipole.[3,4] By measuring the ns-delayed emission times of the fluorescence photons with respect to a short excitation pulse, the excited state lifetime can be obtained which reports on the presence of de-excitation pathways.[5] Emission spectra, obtained by binning each photon by its frequency, can be used to infer the excited state energy landscape of the system.[6,7]

Simultaneous measurements of multiple parameters maximize the information obtained from each single molecule.[8,9] Additionally, analyzing the correlated changes between different variables in a time-dependent fashion on a molecule-by-molecule basis provides insights to dynamic processes that are difficult to extract from ensemble-averaged measurements. For example, the photophysics of fluorescent protein DsRed has been elucidated by simultaneous intensity, lifetime, and emission spectrum measurements.[10]

However, most previous experiments were performed on surfaces where additional heterogeneity could be introduced by the act of immobilization.[11] In many cases, solution phase experiments are preferred. However, in solution, multiparameter measurements of single molecules, although useful, have information limits due to the paucity of detected photons per molecule. Analysis usually involves statistical averaging between many molecular events.[12] Fluorescence lifetimes from freely diffusing molecules during the brief ms-long transit through a tight laser focus have been determined[13,14] but usually with large uncertainties. Full emission spectra of single diffusing molecules have not been determined in solution.

We have developed an experimental platform called the anti-Brownian electrokinetic (ABEL) trap for conducting single-molecule studies in solution with long observation times.[15] The ABEL trap works by real-time position tracking of the fluorescent object, and using microfluidic electrokinetic feedback forces to keep object in the microscope's detection volume. Most recent generations of the trap use rapid beam scanning and Kalman filter-based signal processing schemes for making rapid and accurate feedback decisions.[16,17] With this new design, even objects as small as a single fluorophore have been successfully trapped.[17] Many new insights have been obtained for a number of biological systems in solution ranging from antenna proteins, redox enzymes, transmembrane receptors, and multisubunit enzymes using the ABEL trap;[18−21] for a recent review, see ref 22.

In this paper, we demonstrate and apply multiparameter spectroscopy in solution using the ABEL trap. We first demonstrate trapping of single fluorphores with simultaneous high precision lifetime and emission spectrum determination. Taking advantage of the ability to follow each single molecule for long times, we then characterize the photodynamics of the

Special Issue: Paul F. Barbara Memorial Issue

Received: September 9, 2012
Revised: November 21, 2012
Published: November 30, 2012

dx.doi.org/10.1021/jp308949d | J. Phys. Chem. B 2013, 117, 4641−4648

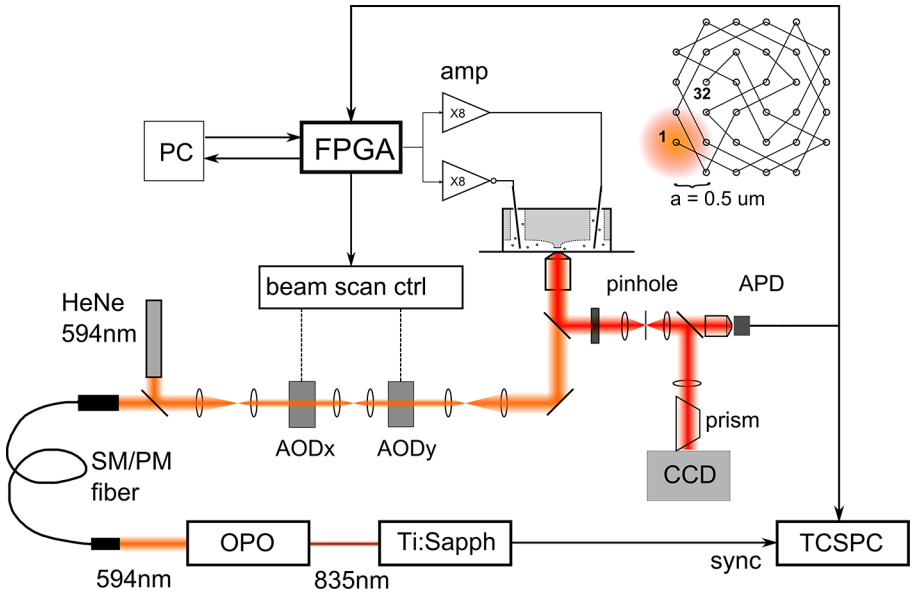

Figure 1. Experimental setup illustrating microfluidic cell, optical excitation, and single-photon detection as well as spectral recording and FPGA-based electrokinetic feedback. A 32-point "knight's tour" scanning pattern (upper right) was used to quickly determine the position of diffusing objects in real time. Both the beam size ($1/e^2$ waist radius) and the spacing of the grid were about 0.5 μm. See the Materials and Methods section for a detailed description. SM/PM = single mode/polarization maintaining.

dye Atto647N in detail, using all information obtained about every single molecule's brightness, lifetime, and emission spectrum. Two other dyes, namely, Atto633 and Alexa647, are also examined by the same method.

MATERIALS AND METHODS

Sample Preparation. All single dye trapping experiments were performed in 1× PBS (pH 7) buffer containing a triplet quencher (1 mM Trolox),[23] a protocatechuate oxygen scavenger system (50 nM protocatechuate-3,4-dioxygenase and 1 mM protocatechuic acid),[24] and 10% glycerol (to avoid rapid sample evaporation during experiments). The final concentration of the dyes ranged between 1 and 5 pM. Dyes (Atto647N and Atto633 (Atto-Tech GMBH), Alexa647 (Invitrogen)) with a *N*-hydroxysuccinimide functional group were used in this study without further purification. To avoid labeling the surface lysines of protocatechuate-3,4-dioxygenase, dye solutions were hydrolyzed by dilution into 1× PBS buffer at ~5 μM concentration and stored at 4 °C overnight before use.

ABEL Trap Algorithm and Microfluidic Environment. To detect the position of the fluorescent object in real time, an excitation beam was scanned on a two-dimensional grid via a "knight's tour" scanning pattern and the beam position at the moment of each photon detection event was recorded as a raw measurement of the object's position (Figure 1). A Kalman filter algorithm[25] then refines the position estimates given previous estimates, applied voltages, and *a priori* knowledge about the object's dynamical parameters. 2D feedback voltages were subsequently calculated, amplified, and applied to the microfluidic channels to induce electrokinetic forces in the thin central region of the trap for approximate cancellation of Brownian motion. All algorithms were implemented on a National Instruments FPGA board (NI 7842R) with an 80 MHz clock rate. Beam scanning was achieved by acousto-optical deflection; the dwell time at each scan point is 600 ns. Feedback delay, defined as the time between photon detection and the output of feedback voltage from the board D/A port, is around 2.5 μs (1.5 μs calculation delay + 1 μs D/A conversion). More technical details can be found in ref 16.

Trapping experiments were performed in an all-quartz microfluidic cell[26] with a channel depth of ~600 nm in the axial *z*-direction. Before loading the sample, the cell was cleaned in an UV-ozone cleaner for 30 min, sonicated in 1 M KOH for 30 min, thoroughly rinsed with nanopure water, and dried by a stream of desiccated N_2. No surface passivation method was needed in this study. Electro-osmosis was determined to be the dominant force in feedback actuation.

Excitation and Detection Optics. As illustrated in Figure 1, CW laser excitation was provided by a 594 nm HeNe laser with random polarization (Meredith). Pulsed light (~200 fs pulses at 78 MHz repetition rate) from a synchronously pumped optical parametric oscillator (Coherent Mira-OPO, pumped by a Coherent 532 nm Verdi-driven Mira-D Ti:sapphire oscillator) tuned to 594 nm was used for time-correlated single photon counting (TCSPC). Excitation light was spectrally filtered by a band-pass filter (Semrock FF01-592/8-25) before impinging on the sample. Fluorescence was collected by a water-immersion objective (Nikon, NA1.3) with the correction collar adjusted to "140 μm" to compensate for spherical aberration induced by the index difference between quartz and glass. A large confocal pinhole that encompassed the whole beam scan pattern (corresponding to about 5 μm in diameter at the sample plane) provided out-of-focus background rejection. The emission signal was then spectrally filtered with a 620−750 nm set of optical filters (Chroma HQ620LP, Semrock 594LP, and Semrock 650/150 BP) and split with a 70:30 ratio between a single-photon counting avalanche photodiode module (EG&G SPCM-AQ-141) and a prism-based spectrometer (see below).

Single-Molecule Fluorescence Emission Measurements. The fluorescence emission spectrum of the trapped single molecule was recorded by dispersing 30% of the collected signal photons via an Amici prism (Edmund Optics, NT42-586)[27] and projected onto an EMCCD camera (Andor

dx.doi.org/10.1021/jp308949d | J. Phys. Chem. B 2013, 117, 4641−4648

DU860E). Pixel-to-wavelength calibration was performed by comparing (peak-matching) the recorded spectrum of a HeNe tube discharge by a commercial spectrometer (Ocean Optics USB4000) and the prism-based setup. Due to the much higher spectral resolution of the commercial spectrometer, its recorded spectrum was convolved with a Gaussian function (σ = 1.8 nm) in the peak-matching process. The resolution of our prism-based spectrometer, determined by the recorded spectral width (1 s.d.) of the single HeNe 594.1 nm line, was about 1.5 nm. Spectral frames were recorded in frame transfer mode with 50 ms exposure time. The "fire" output from the EMCCD was time-tagged in a TCSPC module (Picoquant PicoHarp 300) to provide time markers. In this way, spectral frames were synced in time with traces of intensity and lifetime.

Data Analysis. All data analysis was performed with customized software in Matlab. Before single-molecule identification and extraction steps, the intensity data is preprocessed to determine the background level. First, the photon-by-photon arrival time data is converted to "mcs" trace (counts/bin time) with a 5 ms bin window. A change point (CP) finding algorithm[28] with a large critical value was then performed on the 5 ms binned mcs trace as a smoothing step. A k-means algorithm with N clusters ($N > 3$) subsequently classified every CP bin to a certain cluster. Background is considered to be represented by the cluster with the lowest averaged intensity. With every intensity bin now classified as either background or not, single-molecule events were identified as starting from the first nonbackground bin and ending at the last bin before a background bin. Only nonsticking molecules that last more than 200 ms were selected for further analysis. Sticking events (to quartz surfaces) are easily identified by the presence of nonsymmetric feedback voltages and were rare in this study (<3% for Atto647N and Atto633, <1% for Alexa647).

With selected single molecules, the intensity CP algorithm was performed once more with a small critical value to capture all possible intensity dynamics. Lifetime analysis and emission spectrum analysis were performed on each CP intensity level, defined as data between two adjacent change points.

Spectrum Fitting. After background levels were identified (see above), all spectral frames associated with these levels were averaged to yield the background spectrum. With 594 nm excitation, the background spectrum was dominated by two water Raman peaks around 645 and 750 nm. The spectra from each CP intensity level were averaged, background subtracted, and fitted to a sum of two Gaussians. Emission peaks were determined numerically from the fitted functions.

Lifetime Fitting. Photon arrival delay times with respect to the excitation pulses were histogrammed with a bin width of 80 ps to create the decay histogram, which was fitted with the following functional form:

$$g(t;\tau,c) = (1-\gamma)\left[\mathrm{IRF}(t-c) \otimes \exp\left(-\frac{t}{\tau}\right)\right] + \gamma g_{\mathrm{BG}}(t)$$

where γ is the background fraction, $g_{\mathrm{BG}}(t)$ is the experimentally measured decay histogram from background photons, IRF(t) is the instrument response function, c is the time shift of the IRF during the experiment, and τ is the excited state lifetime. Fitting was performed by a maximum likelihood approach which correctly modeled the Poisson statistics in photon counting.[18,29,30] τ and c are the only two free parameters of the fit. Fitting errors in τ (68% confidence interval) were determined by inversion of the observed Fisher information matrix[31]

$$\Delta\tau = \sqrt{(\mathbf{J}^{-1})_{11}}$$

where $\mathbf{J}$ is the observed Fisher information matrix (the negative of the Hessian matrix during likelihood maximization).

RESULTS

Trapping Single Fluorophores in Solution. Before feedback was switched on, short intensity spikes were observed due to diffusing molecules undergoing transient interactions with the confocal scanning pattern (Figure 2a, left). After feedback was enabled, single dye molecules, upon random diffusion into the beam scanning region, became localized near the center. Due to the time-averaged homogeneous excitation profile provided by the beam scan pattern, near constant emission intensities were observed, exemplified by typical traces shown in Figure 2a. Several experimental observations provided confirmation that the objects trapped were indeed single dye molecules. First, when the feedback is off, the interaction time with the 4 μm scanning pattern, as estimated from the height of the fluorescence spikes, is only several milliseconds, consistent with an object with a large diffusion coefficient ($(4D\Delta t)^{1/2}$ = 2.5 μm for D = 300 μm^2/s, a typical single dye value and Δt = 5 ms). Second, stable trapping of single fluorophores could only be achieved when the detected photon count rate was higher than around 30 kHz, while stable trapping of single-dye labeled proteins (~100 kDa, roughly 8 times slower than a single dye) required a much lower count rate of 3−5 kHz. This is consistent with the design principle of the ABEL trap that an increase of diffusion coefficient by k requires an increase in feedback bandwidth by the same factor in order to maintain comparable trapping strength.[32] Third, the measured fluorescence lifetime and emission spectrum in the trap (see below) were in excellent agreement with the manufacturer's specifica-

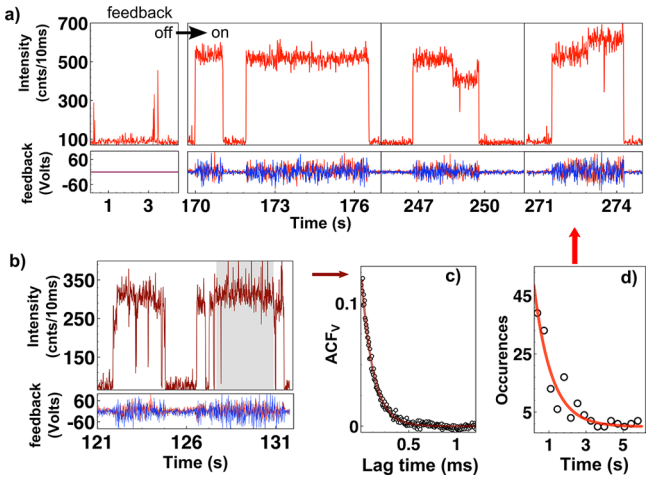

Figure 2. Single fluorophore trapping. (a) Example traces of Atto647N molecules before and after feedback is switched on with feedback voltage records (summed every 10 ms, bottom strip, red: x, blue: y). (b) Example traces of Atto633; infrequent, transient dips were likely due to blinking. (c) Voltage autocorrelation function from the shaded region in part b and fit to an exponential decay with a time constant of 120 μs. (d) Trapping duration histogram of Atto647N and fit to an exponential decay. The average trapping time from this data set is 1.3 s.

dx.doi.org/10.1021/jp308949d | J. Phys. Chem. B 2013, 117, 4641−4648

tions and literature values for the three different dyes (Atto647N, Atto633, and Alexa647) in aqueous solution.

Zero mean, rapidly fluctuating trapping voltage records (Figure 2a and b, bottom) suggest that the long dwell times in the trap are not due to surface sticking. Submillisecond autocorrelation of the applied voltages showed exponentially decaying behavior (with a decay time of ∼100 μs, Figure 2c), further confirming the lack of short-time surface interactions. Since applied voltages are proportional to position estimates, the decay constant of voltage correlation can be used to estimate the trapping strength.[17] Under our experimental conditions (594 nm pulsed light excitation, oxygen removal, and Trolox as the triplet quencher), we achieved the best trapping with Atto647N. An example trace showing trapping of Atto633 (cw excitation) is shown in Figure 2b. In one of the best experimental runs with Atto647N (131 molecules), the average trapping duration is 1.3 s (Figure 2d). We harvested an average of 51 675 photons per single molecule (max, 246 753; median, 32 786).

For the dye Atto647N, some molecules showed one unique intensity level during its residence time, while others switched between different intensity states (Figure 2a). We next investigated these different intensity states in more detail with simultaneous intensity/lifetime/emission spectrum measurements in the ABEL trap.

Simultaneous Measurement of Intensity/Lifetime/Emission Spectrum in the ABEL Trap. For every molecule localized in the ABEL trap, intensity, fluorescence lifetime, and emission spectrum were measured simultaneously. Figure 3b shows an example of multiparameter measurement of a trapped Atto647N molecule. In this particular molecule, only one unique intensity level is present. Intensity is quantified by the number of photon counts per 5 ms and is plotted in red. Intensity autocorrelation (Figure 3e) shows no blinking at short time scales (down to 100 μs). From the time-tagged photons, a fluorescence lifetime trajectory (Figure 3b, blue, left axis) is constructed by successively fitting every 250 photons. The distribution of lifetimes along the intensity level is well-fit by a Gaussian (Figure 3a). The width of the lifetime distribution (s.d. 0.39 ns) is found to be comparable to the average of the fitting error (0.38 ns), suggesting no lifetime dynamics. With a photon counting rate of 52 kHz in this case, lifetime dynamics can be probed with 4.7 ms time resolution with every 250 photons. Autocorrelation analysis of the lifetime trajectory (Figure 3c) was performed and further confirms the absence of significant dynamics. An emission spectrum trajectory, represented by the center of mass of each spectral frame (50 ms time resolution), is plotted in purple (Figure 3b). No apparent spectral dynamics during the residence time of the molecule is observable. Due to the general lack of dynamics of all three parameters within a single intensity level, we pool all the photons during that level and determine its time-average intensity (black line in Figure 3b), lifetime (Figure 3d and blue dotted line in Figure 3b), and spectrum (Figure 3f and purple dotted line in Figure 3b), where the expected presence of a vibrational sideband is evident.

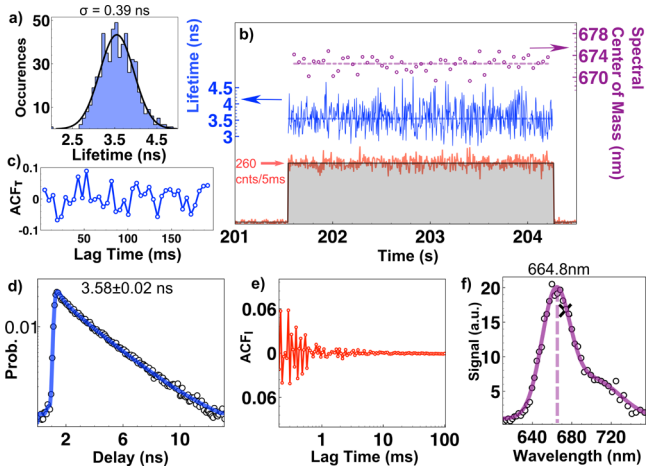

Figure 3. Simultaneous intensity, lifetime, and emission spectrum measurements of a single Atto647N molecule in solution. This molecule contains only one unique intensity level. (a) Histogram of lifetimes (blue trajectory in part b, 250 photon binned) with a Gaussian fit (solid black, standard deviation σ = 0.39 ns). (b) Intensity (red), lifetime (blue), and spectral (purple) trajectories of the trapped Atto647N molecule. Intensity is displayed in 5 ms bins, lifetime is constructed by successive fitting of every 250 photons. Spectrum is represented by the center of mass of each 50 ms spectral frame. (c) Autocorrelation of lifetime, calculated with the 250 photon binned data in part b. (d) Lifetime determined from all photons from the intensity level. (e) Intensity autocorrelation; fluctuation at short time scale is due to beam scanning motion. (f) Emission spectrum determined from all photons from the intensity level. The dashed purple line indicates the peak position. The position of the black cross indicates the center of mass of the spectrum, which is the quantity plotted in part b.

Atto647N Switches between Different Intensity Levels with Distinct Spectra and Lifetimes. A number of Atto647N molecules were observed to switch between distinct intensity levels during their residence in the trap. Figure 4a (red) provides an example of a molecule that visited multiple intensity states. Lifetime (blue) and spectral (purple) dynamics are displayed above the intensity trajectory and are particularly interesting. Here, lifetime is determined for every spectral frame (50 ms) with error bars determined by the Fisher information analysis (Materials and Methods). Within one intensity level, changes in both lifetime and emission spectrum are generally small (except the region following a blinking event at 208 s, where lifetime lingers sometimes below and sometimes above the level average, while no significant changes were present in intensity/spectrum), consistent with the molecule shown in Figure 2. However, abrupt changes in both lifetime and spectrum happen along with an intensity switch. Changes between lifetime and intensity are correlated (decrease in intensity accompanies decrease in lifetime and vice versa), while lifetime and spectrum changes are anticorrelated (red shift accompanies reduction in lifetime and vice versa). A total of three intensity states are present in this particular molecule (exemplified by the color coded regions). Figure 4b–g shows lifetime (blue) and emission spectrum fits of the color coded regions. Notice that the emission spectra from the three levels differ in shape as well.

In order to determine whether this switching behavior is common, we conducted measurements on a total of 683 Atto647N molecules. For every molecule, we identify its intensity levels by the change-point finding algorithm (1153 levels in total). We then extract the fluorescence lifetime and emission peak wavelength of each intensity level and plot it as a point in the intensity-lifetime-emission peak 3D parameter space. Figure 5a–c shows 2D distributions of all the levels as different projections of the 3D parameter space. Three distinct clusters can be identified in intensity/spectrum and intensity/

dx.doi.org/10.1021/jp308949d | J. Phys. Chem. B 2013, 117, 4641–4648

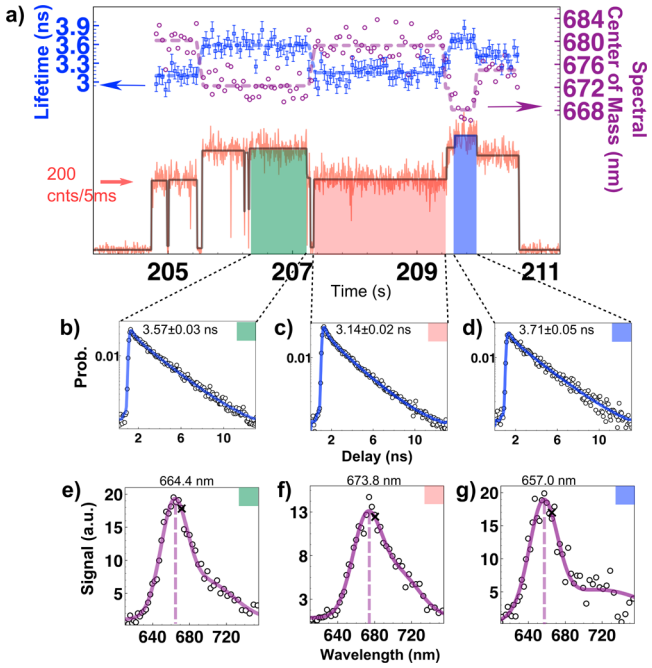

Figure 4. Example of an Atto647N molecule showing dynamics. (a) Intensity, lifetime, and spectral dynamics. Intensity (red) is displayed in 5 ms bins. Both the lifetime (blue) and spectrum (center of mass, purple) are determined from every 50 ms spectral frame. Intensity levels identified by the change-point finding algorithm are drawn in black. (b–d) Fluorescence lifetime determined for each color coded region in part a. (e–g) Emission peaks determined for each color coded region in part a. The different colors correspond to the clusters in Figure 5.

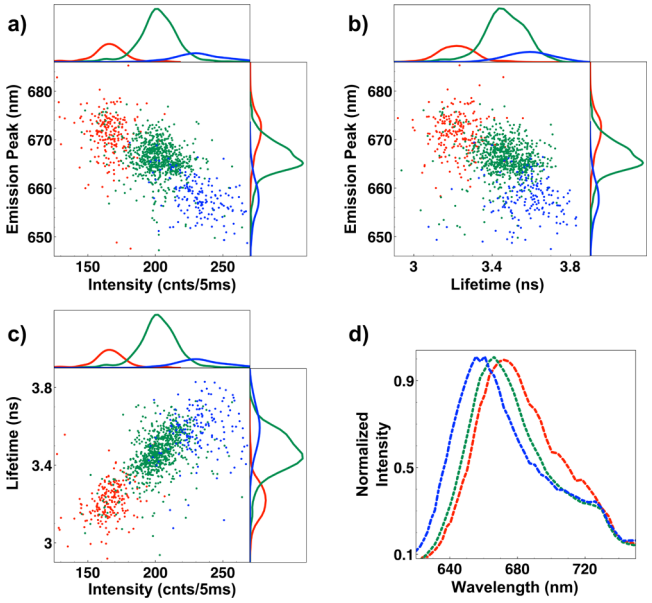

Figure 5. Clustering analysis of Atto647N emission states. (a) Distribution of all the intensity levels, projected onto intensity-spectrum space, (b) lifetime-spectrum space, and (c) intensity-lifetime space; clusters are determined from a 3-D *k*-means algorithm and color coded for clarity. Marginal densities along each variable are shown on the sides. Each curve of the marginal density has an integrated area that is proportional to the total number of levels in the cluster. (d) Average spectrum from each cluster, normalized by the peak. The sharp drop near 745 nm is due to filter cutoff.

lifetime spaces. Representative examples of these states are shown in Figures 4 and 2a. As an attempt to quantitatively describe these clusters, we used the *k*-means algorithm in 3D parameter space to identify and classify all levels into three populations. As a result, the levels are color coded by the cluster to which they belong. Marginal densities of every cluster along each parameter dimension are plotted on the sides of the distribution. Specifically, we have a low-intensity (cluster averaged mean: 165 cnts/5 ms), low-lifetime (3.20 ns) and red-shifted (672 nm) state (red, 19.3% of total levels); a high-intensity (233 cnts/5 ms), high-lifetime (3.60 ns) and blue-shifted (658 nm) state (blue, 15.5%); and finally a state (green, 65.2%) with intermediate intensity (202 cnts/5 ms), lifetime (3.46 ns) and emission peak (667 nm). The most abundant "green" state has properties that are similar to bulk (lifetime 3.5 ns, emission peak 669 nm[33]). Solution phase identification of the "red" and "blue" states is only possible by our new technique. The spread in lifetime and emission peak positions within a cluster are larger than the fitting errors, suggesting additional inhomogeneity within the cluster. Figure 5d shows the cluster averaged spectra of the three states. The "green" and "blue" states are similar in shape despite the ~10 nm shift in peak positions, while the "red" state is broader and has an altered vibronic structure.

State Transitions in Atto647N. Our cluster analysis has unveiled three emission states in Atto647N in solution. From the example in Figure 4 and the ability to follow the same molecule for a long time, we also know that transitions happen between states. To better visualize the state transition, we plot the correlated parameter changes which occur with each identified change point (Figure 6a–c). Every transition is color coded by the ending state. As shown in these plots, the types of

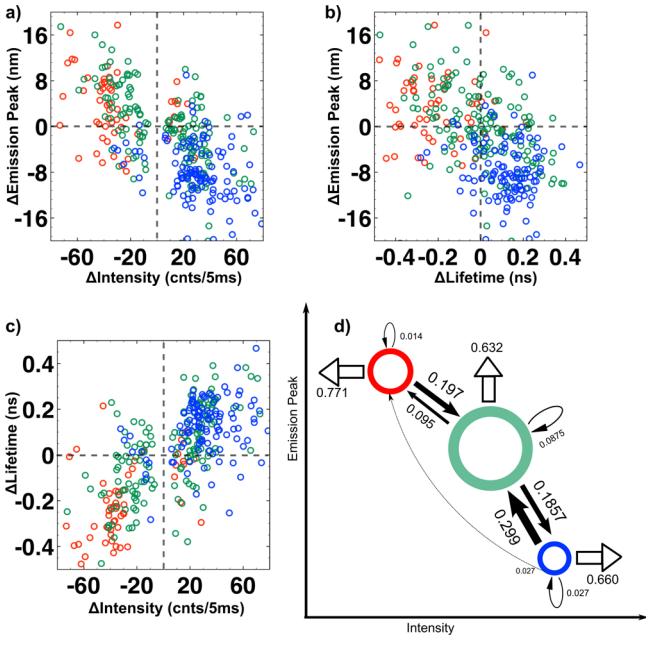

Figure 6. Transitions in single Atto647N molecules. (a) Changes in intensity versus changes in emission peak; positive values indicate red shifts. (b) Changes in lifetime versus changes in emission peak. (c) Changes in intensity versus changes in lifetime. (d) Transition probabilities between states. The relative positions of the three states correspond qualitatively to Figure 5a. Black arrows indicate transitions between states. Unfilled arrows indicate trap loss/photobleaching.

dx.doi.org/10.1021/jp308949d | J. Phys. Chem. B 2013, 117, 4641–4648

transitions seen in Figure 4 are prevalent among Atto647N molecules: upon shifting to the "blue" state, the molecule undergoes an increase in intensity, a blue shift in emission peak, and an increase in lifetime; upon shifting to the "red" state, the molecule undergoes a decrease in intensity, a red shift in emission peak, and a decrease in lifetime. Using all the transitions observed, Figure 6d illustrates the transition probabilities $P(y|x)$, defined as the probability of going into state y when it is at state x. Unfilled arrows indicate photobleaching or trap loss, which is the dominant pathway for all states. Interestingly, "red" and "blue" states do not interconvert and both tend to transition back to the "green" state. From the "green" state, the molecule can go to either "red" or "blue" states, although going to the high-intensity, blue-shifted state is more favorable. Self-transition (indicated by an arrow pointing back to the starting state) of the "green" state is higher than the other two, suggestive of possible substructures within that state.

Rates of Spectral Fluctuation in Solution. It is of practical interest to characterize the time scale of spectral fluctuation of Atto647N in solution. Before we proceed, however, it is worth noting that, in our case, trap loss/photobleaching happens at a rate around 1 s^{-1}, so very long-time dynamics are not sufficiently sampled. Our result should thus be regarded as an upper bound of the rates.

In Figure 7, dwell times before a red/blue spectral shift are histogrammed and fit to exponential decays to extract the rates.

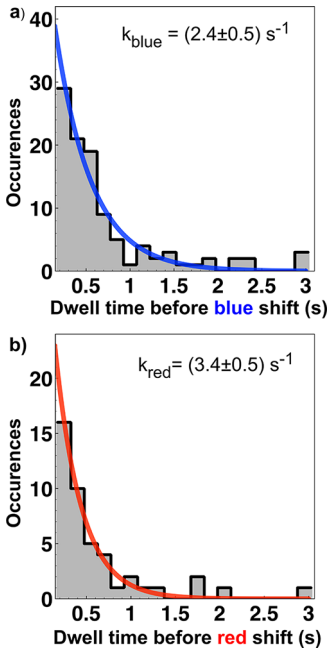

Figure 7. Estimates of the rate of spectral fluctuation in Atto647N. (a) Dwell time histogram before a blue shift is fitted to an exponential decay. (b) Dwell time histogram before a red shift is fitted to an exponential decay.

A spectral shift is defined as when the difference in emission peaks is larger than 1.5 times the maximum fitting error. Slightly higher rates for red-shifting are obtained.

Alexa647 is More Homogeneous. Similar measurements and analysis were performed on Alexa647, a dye with a structure very similar to the widely studied fluorophore, Cy5 (220 molecules, Figure 8a). Unlike Atto647N, only one

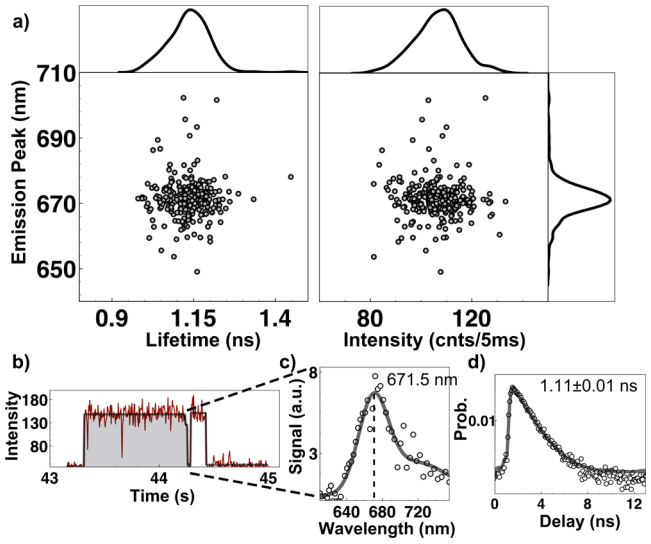

Figure 8. Multiparameter clustering analysis and an example of trapped Alexa647 molecule. (a) Mapping of each intensity level on lifetime-spectrum and intensity-spectrum spaces. A single population is seen. (b) Example of the intensity trajectory of a trapped Alexa647 molecule, its lifetime, and spectrum fits.

population with a relatively narrow emission peak distribution is observed. There is some asymmetry in the lifetime and intensity distributions, but no obvious subpopulations can be identified. The average fluorescence lifetime is determined to be 1.13 ns, consistent with that measured in bulk. The 10% glycerol present in our buffer slightly increases the lifetime of Alexa647 (from 1.0 ns in water).[34] An example intensity trace, together with its spectral and lifetime fits, is shown in Figure 8b–d.

DISCUSSION

The ability to discover and characterize molecule-to-molecule heterogeneity has been one of the most celebrated feats of single-molecule spectroscopy.[35] However, in many cases, heterogeneity may be induced by sample preparation. For instance, when molecules are immobilized on a surface, factors such as differences in dielectric environment, hydrogen bonding network, electrostatic interactions with the surface, molecular orientation, and restricted degrees of rotational freedom might all affect the emission properties of the molecule. One of the great advantages of conducting solution phase measurements with the ABEL trap is the ability to suppress surface-induced artifactual heterogeneity, while harvesting enough photons for precise measurement of intrinsic properties of single molecules. An alternative strategy, encapsulation in a vesicle,[36,37] can provide similar advantages, but the number of molecules which can be studied is larger with the ABEL trap. In our experiments, every molecule experiences the same aqueous environment, orientation and polarization effect are rapidly averaged out by rotational diffusion. Indeed, our measured lifetime/emission peak distributions of Alexa647 are much narrower than previously reported surface immobilized experiments on Cy5.[38] Similar effects of reduced heterogeneity in solution have been observed in the antenna protein allophycocyanin.[18]

The distinct emission states of Atto647N could result from different conformations of the molecule. Previous experiments on another rhodamine, sulforhodamine 101, on surfaces[39,40] reported correlated dynamics of intensity and emission peak. In

dx.doi.org/10.1021/jp308949d | J. Phys. Chem. B 2013, 117, 4641−4648

their case, higher intensity corresponds to a blue shift (~200 cm^{-1}) in emission spectrum. We have observed a similar trend and shifting magnitude for Atto647N in solution. In the case of sulforhodamine 101, Lu et al. found two time scales for spectral fluctuation, a relatively fast decay component of 1.9 s^{-1}, which was independent of excitation power, and a slow component of 0.022 s^{-1}, which had a quasi-linear dependence on excitation power.[41] The fast component was assigned to spontaneous (thermally driven) fluctuations, while the slow component was likely light-induced. We have not done intensity-dependent characterization of the spectral fluctuations of Atto647N, although we made an observation which indicates that transition to the "blue" state is likely light-driven while transition to the "red" state is less so. When molecules first entered the trap (initial level), relative populations were 20.7% (red), 74.2% (green), and 5.1% (blue). However, the relative populations shifted to 19.8% (red), 64.1% (green), and 16.1% (blue) right before molecules left the trap. Many molecules were already in the "red" state, while very few were in the "blue" state before they entered the trap, suggestive of a "red" and "green" only equilibrium before laser illumination. Apparently, interaction with the laser deposited more population to the "blue" state, shifting the equilibrium. It is also possible that, since some molecules are lost from the trap before photobleaching, some of the molecules which first enter the trap had been previously irradiated.

Subtle differences in the shapes of emission spectra are observed for the three states (Figures 4 and 5). Several vibronic sidebands are visible, and their relative contributions compared to the main emission band change for the various states. Although it is not possible in this initial study to fully determine the precise mechanism, these spectral changes might be due to enhanced coupling to certain sets of vibronic modes after slight rearrangement of intramolecular nuclear coordinates. Of course, whatever coordinate changes occur, the overall highly emissive π electron core structure of the molecule is not altered, so one can only surmise that the changes could be due to conformational changes of more distant functional groups.

As noted in the early days of single-molecule spectroscopy, intensity fluctuations associated with spectral changes can be explained by shifts in absorption profile.[42] We have also observed lifetime changes with spectral/intensity changes. In particular, lower intensity, redder states tend to have lower lifetimes, indicating that additional quenching pathways activated after a conformational switch might also play a role in reducing the observed brightness.

Recently, Le Reste et al.[43] noticed that Atto647N, when covalently attached to ssDNA, interconverts slowly between two or more intensity states. The predominant dimmer state is 20% lower in intensity. This finding corresponds well to the "red" state (18.5% dimmer than the "green" state) discovered in our case. Vogelsang et al.[44,45] also mentioned two emission states that are "spectrally distinct but elsewise photophysically similar" when labeled on oligonucleotides. The conversion rates are similar in these studies (approximately tens of seconds) despite order of magnitude differences in excitation power (28 W/cm^2 by Le Reste et al. and 2000 W/cm^2 by Vogelsang et al., both at 638 nm), which also indicates that the transition to the dimmer state is not light driven. Our excitation rate (4000 W/cm^2 at 594 nm) is similar to that used by Vogelsang, but we have observed a much faster conversion rate (~2 s^{-1}). It might be possible that the negatively charged backbone of the oligonucleotides has a stabilizing effect on the conformational switching dynamics of the fluorophore. It is also possible that the rate of dynamics depends on the buffer conditions, especially the oxygen scavenging agent and triplet quencher.

We have conducted similar experiments on Atto633 and found a very similar switching behavior. It is possible that both Atto dyes share similarities in their structure and conformational configurations. While both dyes have become increasingly popular in single-molecule studies due to their excellent brightness/photostability, observation of intrinsic brightness fluctuations of these dyes suggests that care must be exercised when using their intensities as reporters in single-molecule assays.[45−47]

SUMMARY

We have demonstrated simultaneous intensity, lifetime, and spectral measurements of single fluorophores in the ABEL trap. In aqueous solution, such measurements have not been possible previously. Our apparatus is capable of capturing objects as small as a single fluorophore when the photon detection rate exceeds about 30 000 s^{-1}, needed for fast sampling of position dynamics before diffusive escape. The high photon emission rates also allow us to measure fluorescence lifetime and emission spectra with a high time resolution (4.7 ms for lifetime and 50 ms for spectrum in our case). We used the apparatus to study the intrinsic photodynamics of Atto647N, Atto633, and Alexa647.

Three distinct emission states with slightly different intensities, lifetimes, and emission peaks are observed in the dye Atto647N. Transitions are observed to happen between a "bulk-like" state, either to a red-shifted, low intensity, and low lifetime state or to a blue-shifted, high intensity, and high lifetime state. Both forward and backward transitions are observed. We characterized these states in the intensity-lifetime-spectrum parameter space and quantified the transition probabilities between the states. We speculate that these states correspond to slight rearrangements of the fluorophore conformation. Unlike Atto647N, no apparent dynamics are observed in the cyanine dye Alexa647 on the time scale of 1−1000 ms.

Our technique allows an unprecedented amount of information to be obtained for single molecules in solution and will be applicable to the exploration of photodynamics and photophysics for a variety of systems.

AUTHOR INFORMATION

Corresponding Author

*E-mail: wmoerner@stanford.edu. Phone: 650-723-1727. Fax: 650-725-0259.

Notes

The authors declare no competing financial interest.

ACKNOWLEDGMENTS

We thank Dr. Randall Goldsmith for initially designing the Amici prism setup and for prism calibration and alignment. The authors acknowledge the Division of Chemical Sciences, Geosciences, and Biosciences, Office of Basic Energy Sciences of the U.S. Department of Energy through Grant DE-FG02-07ER15892 for funding the development of the apparatus used in this study.

REFERENCES

(1) Claridge, S. A.; Schwartz, J. J.; Weiss, P. S. *ACS Nano* **2011**, *5*, 693−729.
(2) Moerner, W. E.; Fromm, D. P. *Rev. Sci. Instrum.* **2003**, *74*, 3597−3619.
(3) Rosenberg, S. A.; Quinlan, M. E.; Forkey, J. N.; Goldman, Y. E. *Acc. Chem. Res.* **2005**, *38*, 583−593.
(4) Sosa, H.; Peterman, E. J. G.; Moerner, W. E.; Goldstein, L. S. B. *Nat. Struct. Biol.* **2001**, *8*, 540−544.
(5) Yang, H.; Luo, G.; Karnchanaphanurach, P.; Louie, T.; Rech, I.; Cova, S.; Xun, L.; Xie, X. S. *Science* **2003**, *302*, 262−266.
(6) van Oijen, A. M.; Ketelaars, M.; Kohler, J.; Aartsma, T. J.; Schmidt, J. *Science* **1999**, *285*, 400−402.
(7) Blum, C.; Stracke, F.; Becker, S.; Mullen, K.; Meixner, A. J. *J. Phys. Chem. A* **2001**, *105*, 6983−6990.
(8) Macklin, J. J.; Trautman, J. K.; Harris, T. D.; Brus, L. E. *Science* **1996**, *272*, 255−258.
(9) Vanden Bout, D. A.; Yip, W. T.; Hu, D.; Fu, D. K.; Swager, T. M.; Barbara, P. F. *Science* **1997**, *277*, 1074−1077.
(10) Cotlet, M.; Hofkens, J.; Habuchi, S.; Dirix, G.; Van Guyse, M.; Michiels, J.; Vanderleyden, J.; De Schryver, F. C. *Proc. Natl. Acad. Sci. U.S.A.* **2001**, *98*, 14398−14403.
(11) Friedel, M.; Baumketner, A.; Shea, J. E. *Proc. Natl. Acad. Sci. U.S.A.* **2006**, *103*, 8396−8401.
(12) Chen, Y.; Müller, J. D.; So, P. T.; Gratton, E. *Biophys. J.* **1999**, *77*, 553−567.
(13) Edman, L.; Mets, U.; Riger, R. *Proc. Natl. Acad. Sci. U.S.A.* **1996**, *93*, 6710−6715.
(14) Eggeling, C.; Fries, J. R.; Brand, L.; Gunther, R.; Seidel, C. A. M. *Proc. Natl. Acad. Sci. U.S.A.* **1998**, *95*, 1556−1561.
(15) Cohen, A. E.; Moerner, W. E. *Appl. Phys. Lett.* **2005**, *86*, 093109.
(16) Wang, Q.; Moerner, W. E. *ACS Nano* **2011**, *5*, 5792−5799.
(17) Fields, A. P.; Cohen, A. E. *Proc. Natl. Acad. Sci. U.S.A.* **2011**, *108*, 8937−8942.
(18) Goldsmith, R. H.; Moerner, W. E. *Nat. Chem.* **2010**, *2*, 179−186.
(19) Goldsmith, R. H.; Tabares, L. C.; Kostrz, D.; Dennison, C.; Aartsma, T. J.; Canters, G. W.; Moerner, W. E. *Proc. Natl. Acad. Sci. U.S.A.* **2011**, *108*, 17269−17274.
(20) Jiang, Y.; Douglas, N. R.; Conley, N. R.; Miller, E. J.; Frydman, J.; Moerner, W. E. *Proc. Natl. Acad. Sci. U.S.A.* **2011**, *108*, 16962−16967.
(21) Bockenhauer, S.; Fuerstenberg, A.; Yao, J. Y.; Kobilka, B. K.; Moerner, W. E. *J. Phys. Chem. B* **2011**, *115*, 13328−13338.
(22) Wang, Q.; Goldsmith, R. H.; Jiang, Y.; Bockenhauer, S. D.; Moerner, W. E. *Acc. Chem. Res.* **2012**, *45*, 1955−1964.
(23) Rasnik, I.; McKinney, S. A.; Ha, T. *Nat. Methods* **2006**, *3*, 891−893.
(24) Aitken, C. E.; Marshall, R. A.; Puglisi, J. D. *Biophys. J.* **2008**, *94*, 1826−1835.
(25) Wang, Q.; Moerner, W. E. *Appl. Phys. B: Lasers Opt.* **2010**, *99*, 23−30.
(26) Cohen, A. E.; Moerner, W. E. *Opt. Express* **2008**, *16*, 6941−6956.
(27) Wörmke, S.; Mackowski, S.; Brotosudarmo, T. H. P.; Brauchle, C.; Garcia, A.; Braun, P.; Scheer, H.; Hofmann, E. *Appl. Phys. Lett.* **2007**, *90*, 193901.
(28) Watkins, L. P.; Yang, H. *J. Phys. Chem. B* **2005**, *109*, 617−628.
(29) Zander, C.; Sauer, M.; Drexhage, K. H.; Ko, D. S.; Schulz, A.; Wolfrum, J.; Brand, L.; Eggeling, C.; Seidel, C. A. M. *Appl. Phys. B* **1996**, *63*, 517−523.
(30) Brand, L.; Eggeling, C.; Zander, C.; Drexhage, K. H.; Seidel, C. A. M. *J. Phys. Chem. A* **1997**, *101*, 4313−4321.
(31) Pawitan, Y. *In All Likelihood: Statistical Modeling and Inference Using Likelihood*; Clarendon Press: Oxford, U.K., 2001; p 528.
(32) Moerner, W. E. *Proc. Natl. Acad. Sci. U.S.A.* **2007**, *104*, 12596−12602.
(33) Kolmakov, K.; Belov, V. N.; Bierwagen, J.; Ringemann, C.; Müller, V.; Eggeling, C.; Hell, S. W. *Chem.—Eur. J.* **2010**, *16*, 158−166.
(34) Buschmann, V.; Weston, K. D.; Sauer, M. *Bioconjugate Chem.* **2003**, *14*, 195−204.
(35) Moerner, W. E. In *Single-Molecule Optical Spectroscopy and Imaging: From Early Steps to Recent Advances*; Gräslund, A., Rigler, R., Widengren, J., Eds.; Single Molecule Spectroscopy in Chemistry, Physics and Biology: Nobel Symposium 138 Proceedings; Springer-Verlag: Berlin, 2009; pp 25−60.
(36) Benitez, J. J.; Keller, A. M.; Ochieng, P.; Yatsunyk, L. A.; Huffman, D. L.; Rosenzweig, A. C.; Chen, P. *J. Am. Chem. Soc.* **2009**, *131*, 871−871.
(37) Cisse, I.; Okumus, B.; Joo, C.; Ha, T. *Proc. Natl. Acad. Sci. U.S.A.* **2007**, *104*, 12646−12650.
(38) Tinnefeld, P.; Herten, D.-P.; Sauer, M. *J. Phys. Chem. A* **2001**, *105*, 7989−8003.
(39) Lu, H. P.; Xie, X. S. *Nature* **1997**, *385*, 143−146.
(40) Yip, W. T.; Hu, D.; Yu, J.; Vanden Bout, D. A.; Barbara, P. F. *J. Phys. Chem. A* **1998**, *102*, 7564−7575.
(41) Lu, H. P.; Xun, L.; Xie, X. S. *Science* **1998**, *282*, 1877−1882.
(42) Trautman, J. K.; Macklin, J. J.; Brus, L. E.; Betzig, E. *Nature* **1994**, *369*, 40−42.
(43) Le Reste, L.; Hohlbein, J.; Gryte, K.; Kapanidis, A. N. *Biophys. J.* **2012**, *102*, 2658−2668.
(44) Vogelsang, J.; Kasper, R.; Steinhauer, C.; Person, B.; Heilemann, M.; Sauer, M.; Tinnefeld, P. *Angew. Chem., Int. Ed.* **2008**, *47*, 5465−5469.
(45) Ha, T.; Tinnefeld, P. *Annu. Rev. Phys. Chem.* **2012**, *63*, 595−617.
(46) Di Fiori, N.; Meller, A. *Biophys. J.* **2010**, *98*, 2265−2272.
(47) Chung, H. S.; Louis, J. M.; Eaton, W. A. *Biophys. J.* **2010**, *98*, 696−706.